51st AIAA Aerospace Sciences Meeting including the New Horizons Forum and Aerospace Exposition
07 - 10 January 2013, Grapevine (Dallas/Ft. Worth Region), Texas

AIAA 2013-0026

Uncertainty Quantification for Mars Entry, Descent, and Landing Reconstruction Using Adaptive Filtering

Soumyo Dutta* and Robert D. Braun†
Georgia Institute of Technology, Atlanta, GA, 30332-1510, USA
and
Christopher D. Karlgaard‡
Analytical Mechanics Associates, Inc., Hampton, VA, 23666-1568, USA

Mars entry, descent, and landing (EDL) trajectories are highly dependent on the vehicle's aerodynamics and the planet's atmospheric properties during the day-of-flight. A majority of previous EDL trajectory and atmosphere reconstruction analyses do not simultaneously estimate the flight trajectory and the uncertainties in the models. Adaptive filtering techniques, when combined with the traditional trajectory estimation methods, can improve the knowledge of the aerodynamic coefficients and atmospheric properties, while also estimating a realistic confidence interval for these parameters. Simulated datasets with known truth data are used in this study to show the improvement in state and uncertainty estimation by using adaptive filtering techniques. Such a methodology can then be implemented on existing and future EDL datasets to determine the aerodynamic and atmospheric uncertainties and improve engineering design tools.

Nomenclature

A	Process equation Jacobian matrix w.r.t. the state vector
B	Process equation Jacobian matrix w.r.t. the noise vector
C	Coefficient (see subscripts)
F	Force, N
f	Process equation
g	Gravity, m/s^2
H	Measurement sensitivity matrix
h	Measurement equation
I	Identity matrix
K	Kalman gain
Kn	Knudsen number
L	Batch size for measurement noise covariance calculation
$M_{v,b}$	Rotation matrix, vehicle-carried local horizontal to body frame
m	Mass, kg
N	Batch size for state noise covariance calculation
P	State covariance matrix
p	Pressure, Pa.
q_i	Quaternion between local horizontal and body frame, $i = 0, ..., 3$
Q	State noise covariance matrix
R	Measurement covariance matrix
r	Planetary radius (planet-centric), m
t	Time, s

*Graduate Research Assistant, Daniel Guggenheim School of Aerospace Engineering, AIAA Student Member.
†David & Andrew Lewis Professor of Space Technology, Daniel Guggenheim School of Aerospace Engineering, AIAA Fellow.
‡Supervising Engineer, AIAA Senior Member.

V	Velocity (planet-relative), m/s
v	Measurement noise vector
w	State noise vector
x	State vector
y	Measurement vector
α	Angle of attack, rad
β	Sideslip angle, rad
γ	Flight path angle (planet-relative), rad
θ	Longitude, rad
ν	Bank angle, rad
ρ	Atmospheric density, kg/m^3
ϕ	Latitude (planet-centric), rad
ψ	Heading angle (planet-relative), rad
ω	Rotation rate, rad/s

Subscript

0	Initial condition
A	Axial force
i	State index
j	Increment for adaptive filter
k	Time increment
l	Roll moment
m	Pitch moment
N	Normal force
n	Yaw moment
T	Tangential force
t	Total condition
x, y, z	Body frames
Y	Side force
∞	Freestream condition

Superscript

T	Transpose
$\bar{}$	Nominal estimate
$\hat{}$	Best estimate

I. Introduction

MARS entry, descent, and landing (EDL) trajectories and the Martian atmospheric properties have been reconstructed from all past U.S. missions. All of these missions have had the same entry body geometry (70 deg. sphere-cone) and have utilized the same supersonic parachute configuration (Disk-gap-band), but the aerodynamic coefficients of these systems remain uncertain. Moreover, the Martian atmosphere is highly variable, thus adding to the uncertainty.

Previous trajectory reconstructions have either largely ignored quantifying the uncertainties surrounding the atmosphere and aerodynamic parameters or have assumed a known value of one of these parameters in order to estimate the state and uncertainty of the other terms. Moreover, as trajectory propagation is highly dependent on the vehicle aerodynamics and atmospheric properties, the uncertainties in these two properties will increase the uncertainty in the trajectory.

Adaptive filtering techniques, developed in the 1960's, have been used in signal processing and inertial guidance and navigation applications for situations where the *a priori* knowledge of the vehicle's model and sensor data uncertainties are unknown. Adaptive filters used in conjunction with statistical filters, like the Extended Kalman filter (EKF), can reconstruct the filter state while also estimating the model and sensor data uncertainties. Since the Mars EDL trajectory reconstruction process is an estimation process using sensor data on-board the vehicles, this study proposes using adaptive filtering to reconstruct the vehicle's trajectory, aerodynamic coefficients, atmospheric parameters, and their uncertainties. A simulated

dataset, where the truth is known, will be used to compare reconstruction process using non-adaptive noise characterization, such as the EKF where the model and sensor errors are assumed to be known, to an estimation process where such error statistics are calculated on-line by the filter.

II. Motivation

A major objective for the reconstruction of Mars EDL flight data is to verify the performance of the vehicle and quantify any off-nominal behavior. It is also useful if the reconstruction methods can quantify uncertainty in the estimated parameters that can be used in the design process. Pre-flight uncertainty analysis has been performed for most past Mars EDL missions, and these show that among a long list of design parameters, two major sources of uncertainties lie in the knowledge of the aerodynamic coefficients of the vehicle and the atmospheric profile the vehicle will encounter.[1] For example, typical uncertainties associated with a Mars EDL vehicle's aerodynamics are summarized in Table 1; however, these uncertainties have been quantified based on Computational Fluid Dynamics (CFD) tools, wind tunnel and ballistic range data, or engineering judgment not reconstruction of flight data.

Table 1: Static Aerodynamic Coefficient Uncertainty for Recent U.S. Mars EDL Vehicles.[2,3]

Phoenix†	C_A	C_N, C_Y	C_m	C_n	C_l
$Kn \geq 0.1$	$\pm 5\%$	± 0.01	$\pm 0.005, \pm 20\%$	$\pm 0.005, \pm 20\%$	N/A
Mach $\geq$ 10*	$\pm 3\%$	± 0.01	$\pm 0.002, \pm 20\%$	$\pm 0.002, \pm 20\%$	1.24×10^{-6}
Mach $\leq$ 5*	$\pm 10\%$	± 0.01	$\pm 0.005, \pm 20\%$	$\pm 0.005, \pm 20\%$	1.24×10^{-6}
MSL†	C_A	C_N, C_Y	C_m	C_n	C_l
$Kn \geq 0.1$	$\pm 5\%$	$\pm 0.01, \pm 10\%$	$\pm 0.005, \pm 20\%$	$\pm 0.005, \pm 20\%$	0.0005
Mach $\geq$ 10*	$\pm 3\%$	$\pm 0.01, \pm 10\%$	$\pm 0.006, \pm 20\%$	$\pm 0.003, \pm 20\%$	0.000219
Mach $\leq$ 5*	$\pm 10\%$	$\pm 0.01, \pm 10\%$	$\pm 0.005, \pm 20\%$	$\pm 0.005, \pm 20\%$	0.00023

*Uncertainty values are linearly blended between regimes.

†Uncertainty model consists of an adder and then a multiplier (Ref. 2).

Gaussian distribution is assumed for the uncertainties listed above.

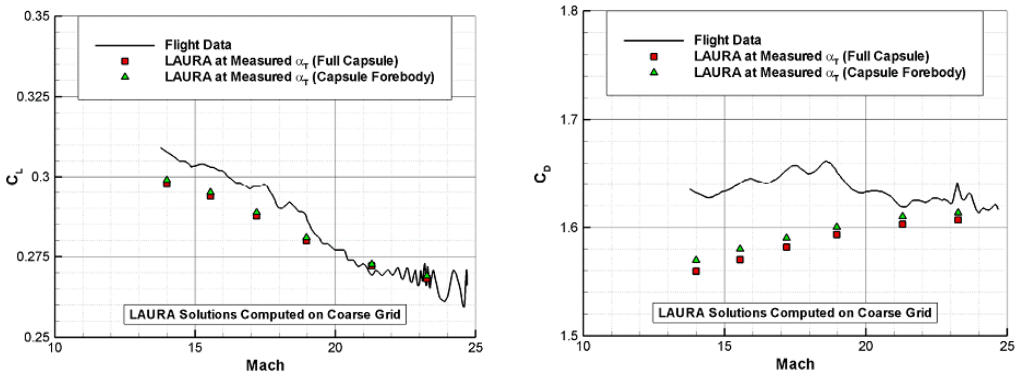

(a) Lift Force Coefficient (b) Drag Force Coefficient

Figure 1: Comparison of Viking lander 1 aerodynamic coefficients based on flight data and CFD tools.[4]

Flight data from the two Viking landers provided in situ atmospheric pressure measurements over the vehicle forebody during EDL and the reconstructed total angle of attack (α_t), lift, and drag coefficients histories provide a benchmark for comparison to the aerodynamic database (shown in Fig. 1).[4] Comparisons of predicted aerodynamic coefficients between state-of-the-art CFD codes and past flight data show that significant uncertainties still exist. These discrepancies underscore the need of using flight data and the reconstructed uncertainties for model verification and improvement.

Another significant source of uncertainty in Mars EDL trajectories is the atmospheric properties of Mars on the day of the flight (see Fig. 2). Large variations in the atmosphere due to the seasons, the amount

of dust particles, and other weather-related events make the prediction of freestream density, pressure, and temperature uncertain. For example, looking at Fig. 2a, one can see large variations in density from the nominal prediction, while Fig. 2b shows how such uncertainty can effect the propagated trajectory. Similar uncertainty in the atmospheric profile knowledge exists for other parameters in the Mars atmospheric models like winds.[5–9]

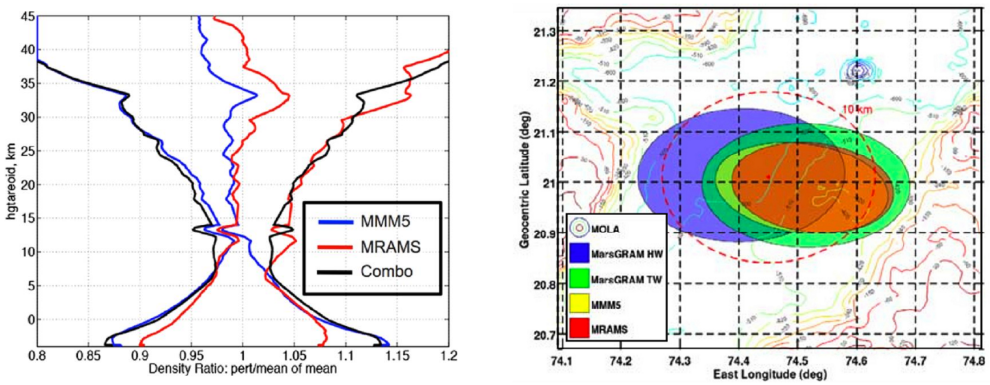

(a) Possible density profiles for MSL.[8] (b) MSL footprints for different atmospheres.[9]

Figure 2: Atmospheric uncertainty's effect on EDL vehicle design.

Additionally, the data taken by Mars EDL vehicles often do not improve the observability of parameters of interest, such as the vehicle aerodynamics and atmosphere. Table 2 summarizes the type of data taken by the successful U.S. missions, and one can see that for most U.S. Mars missions, the on-board data consist of inertial measurement unit (IMU) information, which by itself does not provide any way of estimating aerodynamics and atmospheric properties independently.[10] However, on-board pressure distribution information from Flush Airdata Systems (FADS) like that on the Viking landers and the Mars Science Laboratory (MSL) mission do provide another independent source of information to separate aerodynamic and atmospheric uncertainties.[11]

Table 2: EDL-related measurements taken by U.S. Martian missions.

Measurements	Vikings[a]	Pathfinder[b]	MERs[c]	Phoenix[d]	MSL[e]
Accelerometer	X	X	X	X	X
Thee-axis gyroscope	X		X	X	X
Radar altimeter[f]	X	X	X	X	X
Pressure (during EDL)	X[f]	X[g]			X

Notes: [a]Ref. 12, 13 [b]Ref. 14, 15 [c] Mars Exploration Rovers[16,17] [d]Ref. 18, 19 [e]Ref. 11, 20

[f] Viking pressure and temperature data were found to be inconsistent for conclusive analysis.

[g] Pathfinder only took pressure measurements during subsonic parachute descent.

As discussed later, Adaptive Filters can estimate parameters of interest and their uncertainties while automatically adjusting statistics needed to filter noise in the dynamics. For Mars EDL reconstructions where there is large uncertainty in the process dynamics, especially due to atmospheric and aerodynamic properties, this adaptive estimation of the noise by adaptive filters promises significant improvement in reconstruction applications.

III. Adaptive Filtering Background

The Kalman filter has been a standard approach for trajectory reconstruction in support of experimental flight vehicles and planetary entry performance analysis. A few examples are provided in Refs. 10, 13, 14, 21–32. The Kalman filter allows one to estimate the state vector of interest along with statistics about the estimated quantity, such as uncertainty in the estimate.

A key assumption inherent to the Kalman filter is that the process and measurement noise covariance

matrices are known. If these assumed parameters of the distribution differ greatly from the true parameters, then the filter can exhibit large errors, inconsistency, and possibly divergence[33] in nonlinear problems. Such uncertainties in the covariance matrices are particularly problematic for planetary EDL reconstruction since the atmospheric and aerodynamic uncertainties are not well known. This can be due to many reasons, including limited measurement information for a highly variable atmosphere, aerodynamic data that are acquired in Earth-based wind tunnels with atmospheric chemical compositions different from flight conditions, or the use of aerodynamic predictions that are based on CFD with potential modeling errors. Additionally, trajectory measurement sensors go through launch loads and a long coast period with potentially drastic thermal changes, which could introduce a shift in the assumed calibration.

Adaptive filtering techniques have been frequently used in cases where the noise statistics are estimated along with the state in order to reduce the possibility of divergence of the filter and to improve the estimation performance in the presence of unknown statistics of the underlying noise distributions. These situations are summarized below and are classified according to the four basic techniques suggested in an early review article by Mehra:[34] Bayesian, maximum likelihood, correlation matching, and covariance matching methods.

A. Bayesian, Maximum Likelihood, and Correlation Matching

The Bayesian technique of adaptive filtering involves estimating a set of unknown parameters of interest, which include the state vector, the state covariance matrix, and elements of the process and measurement noise matrices, from a given state of data by attempting to recreate the *a posteriori* distribution. The maximum likelihood technique is similar to the Bayesian technique, since it too attempts to estimate a similar set of unknown parameters of interest using the *a posteriori* distribution, albeit by attempting to maximize the likelihood of this distribution for certain select conditions. The similarities between the two techniques mean that often the underlying equations are the same. Additionally, the Bayesian and maximum likelihood techniques become extremely complicated as the dimension of the measurement noise and process noise covariances matrices increase, since they both involve the calculation of multiple difference equations that increase rapidly in number with the number of elements being estimated.[34] In practice, the Bayesian and maximum likelihood approaches are both simplified into a problem of estimating the Kalman gain matrix directly, which reduces the problem's computational complexity but does not directly permit the evaluation of the sensor performance or the model uncertainty, which are parameters of interest for Mars EDL reconstruction.

A subset of the Bayesian approach introduced by Magill[35] has become known as Multiple Model Adaptive Estimation (MMAE). MMAE utilizes a bank of filters, each with a different hypothesis of the system's model. The outputs of these filters are blended together via a weighted average or some other logic to produce the state estimate. If one of the filters implemented has a closer match to the true statistics, then its weight will tend towards unity. However, this approach has a high computational cost associated with implementing the filter bank, and the implicit assumption is that the true statistics are within the range of the hypotheses. Also, Mehra[34] implies that this approach can sometimes be problematic for identification of the process noise covariance.

The correlation matching technique operates by attempting to correlate the observed output of a system to the unknown noise covariances. These methods can be developed using either the autocorrelation of the output or that of the residuals. The approach using the output is generally more restrictive, so in practice usually the residuals-based approach is preferred. In both cases, the estimates of the process noise covariance are not unique and, moreover, they can only be computed in steady state conditions. Thus, this technique is not useful for the reconstruction of a time-varying signal from a vehicle performing EDL.

B. Covariance Matching

The covariance matching technique is an appealing approach in which the measurement noise and process noise covariances are determined in such a way that the true residual covariance matches the theoretically predicted covariance. The true residual covariance is approximated in real time using the sample covariance, over some finite window of stored residuals. The solution provided by Mehra[34] leads to a non-unique estimate of the process noise covariance, as with the correlation matching method. For this reason, Mehra states that this approach has exhibited best success when the process noise covariance is known and one only wishes to solve for the measurement noise covariance. An example of this approach is given in Ref. 36.

The covariance matching technique is expanded by Myers and Tapley in Ref. 37. In this approach, the authors are able to determine explicit solutions for both the process noise and the measurement noise covariances by using empirical estimators based on the sample covariance for a finite window of stored observations. Myers and Tapley also introduce a fading memory weighting parameter in which more recent observations receive more weight than the older observations. The estimators are derived in batch form, but are manipulated into a recursive form suitable for real-time implementation. The approach is not computationally intensive, requiring only 12% more cost than the standard EKF in one sample problem.

Special cases of the Myers-Tapley method appear in the literature. For example, Maybeck et al.[38] and Whitmore and Leondes[39] propose a covariance matching method to estimate only the process noise covariance matrix, assuming the measurement noise covariance is known. In contrast, Hull et al.[40] devise a special case of the Myers-Tapley method in which the process noise covariance is known and the measurement noise covariance is estimated in real time.

C. Use in Reconstruction Applications

Few authors have considered the use of adaptive filtering techniques for trajectory reconstruction. Chu et al.[41] develop a recursive maximum likelihood adaptive filter and Mendonca et al.[42] implement a covariance matching approach for estimation of both the process and measurement noise covariance matrices for aircraft flight path reconstruction. In both approaches, IMU measurements are used to replace the detailed system models based on the vehicle aerodynamics, thus the process noise model uncertainty estimation amounts to estimating the uncertainties of the accelerometer and gyroscope measurements. The vehicle aerodynamic uncertainties are not addressed in these formulations.

Marschke et al.[43] make use of a MMAE approach for Mars entry navigation. In this approach, three filters are implemented with different state dimensions associated with the estimation of various IMU systematic error parameters. This work is geared toward real-time on-board navigation and so the authors propose a small number of filters. The work does not consider the case of unknown process or measurement noise statistics and thus is unsuitable for the problem of uncertainty quantification.

Adaptive filtering, especially the covariance matching technique, shows great promise for EDL reconstruction, for which often both the process noise and measurement noise statistics are unknown. Additionally, to the best knowledge of the authors, no example in the literature has applied the covariance matching technique for EDL reconstruction.

IV. Methodology

In this study, a simulated EDL trajectory has been used to gauge the efficacy of the adaptive filter reconstruction methodology. The methodology is able to incorporate typical Mars EDL measurements, such as IMU data, FADS data, and radar altimeter data, to reconstruct trajectory, atmospheric parameters, and aerodynamic coefficients.

A. Process Equations

Equations of motion, as seen in Eqs. (1), are the process equations used to propagate the estimate of the states in time.[44] The matrix $M_{v,b}$, which is solely a function of the quaternion, defines the rotation from the local horizontal frame to the body frame and is defined in the literature.[45] The planetary rotation rate is ω_{Mars} and the angular rates in the body frame, ω_x, ω_y, and ω_z, come from the on-board gyroscopes, while g is the altitude-dependent gravitational acceleration based on a spherical mass distribution. F_N and F_T represent the normal (lift) and tangential (drag) forces in the body axis and lift modulation is modeled in the equations using a bank angle (ν). The dynamical equations for the freestream pressure and density are derived from the hydrostatic equation and the perfect gas law and the derivation is described in Refs. 26 and 31.

$$\dot{r} = V \sin\gamma \tag{1a}$$

$$\dot{\phi} = \frac{V \cos\gamma \sin\psi}{r} \tag{1b}$$

$$\dot{\theta} = \frac{V \cos\gamma \cos\psi}{r \cos\phi} \tag{1c}$$

$$\dot{V} = \frac{F_T}{m} - g \sin\gamma + \omega_{Mars}^2 r \cos\phi \left(\sin\gamma \cos\phi - \cos\gamma \sin\phi \sin\psi\right) \tag{1d}$$

$$\dot{\gamma} = \frac{1}{V}\left[\frac{F_N \cos\nu}{m} - g\cos\gamma + \frac{V^2}{r}\cos\gamma + 2\omega_{Mars} V \cos\phi\cos\psi \right.$$
$$\left. + \omega_{Mars}^2 r \cos\phi \left(\cos\gamma\cos\phi + \sin\gamma\sin\phi\sin\psi\right)\right] \tag{1e}$$

$$\dot{\psi} = \frac{1}{V}\left[\frac{F_N \sin\nu}{m\cos\gamma} - \frac{V^2}{r}\cos\gamma\cos\psi\tan\phi + 2\omega_{Mars} V \left(\tan\gamma\cos\phi\sin\psi - \sin\phi\right) \right.$$
$$\left. - \frac{\omega_{Mars}^2 r}{\cos\gamma}\sin\phi\cos\phi\cos\psi\right] \tag{1f}$$

$$\dot{p_\infty} = -\rho_\infty g V \sin\gamma \tag{1g}$$

$$\dot{\rho_\infty} = -\frac{\rho_\infty^2 g V \sin\gamma}{p_\infty} \tag{1h}$$

$$\begin{bmatrix} \dot{q_0} \\ \dot{q_1} \\ \dot{q_2} \\ \dot{q_3} \end{bmatrix} = \frac{1}{2}\begin{bmatrix} -q_1 & -q_2 & -q_3 \\ q_0 & -q_3 & q_2 \\ q_3 & q_0 & -q_1 \\ -q_2 & q_1 & q_0 \end{bmatrix}\left[\begin{bmatrix} \omega_x \\ \omega_y \\ \omega_z \end{bmatrix} - \frac{1}{r} M_{v,b}\begin{bmatrix} V\cos\gamma\cos\psi \\ -V\cos\gamma\sin\psi \\ -V\cos\gamma\cos\psi\tan\phi \end{bmatrix}\right] \tag{1i}$$

B. Extended Kalman filter and traditional reconstruction

An extended Kalman filter is a modification of the linear Kalman filter. The algorithm for this well-known filter is summarized below:[46]

1. Initialize the state vector and the state covariance matrix at time $t_{k-1} = t_0$ and let $k = 1$, where k is an index of the epoch when a measurement is first available.
2. Read in the measurement at time t_k.
3. Calculate a nominal state ($\bar{x}_k$) at time t_k by integrating the non-linear equations of motions (Eqs. (1)) with $\hat{x}_{k-1}$ as the initial condition.
4. Calculate the nominal state covariance matrix ($\bar{P}_k$) by integrating the Riccati equations (Eq. (2a)) using $\hat{P}_{k-1}$ as the initial condition.
5. Calculate the measurement residual vector (y_k), the measurement sensitivity matrix (H_k), and the Kalman gain (K_k) using the nominal state and state covariance (Eq. (2b)).
6. Calculate the best estimate of the state ($\hat{x}_k$) and state covariance ($\hat{P}_k$) using Eqs. (2c) and (2d).
7. Increment counter k and go back to step 2 until measurements at all times have been processed.

$$\dot{P} = AP + PA^T + BQB^T \tag{2a}$$

$$K_k = \bar{P}_k H_k^T \left(H_k \bar{P}_k H_k^T + R_k\right)^{-1} \tag{2b}$$

$$\hat{x}_k = \bar{x}_k + K_k \left(y_k - h\left(\bar{x}_k\right)\right) \tag{2c}$$

$$\hat{P}_k = (I - K_k H_K)\bar{P}_k (I - K_k H_k)^T + K_k R_k K_k^T \tag{2d}$$

A is the Jacobian of the equations of motion with respect to the state vector, B is the Jacobian of the equations of state with respect to the state noise vector, and I is the identity matrix. The measurement

covariance matrix ($R = E(vv^T)$) based on the measurement noise (v) is defined at time k and information from pre-flight sensor calibration information is typically used for this matrix. The process noise covariance ($Q = E(ww^T)$) based on the process noise (w) is typically based on experimentation or pre-flight modeling errors. For Mars EDL trajectory reconstruction, these two types of matrices have the largest uncertainties. The EKF assumes *a priori* knowledge of the R and Q noise matrices; however, for Mars EDL applications, the R matrix might involve *a priori* known bias, scaling, and calibration information, but the Q matrix can include *a priori* unknown aerodynamic and atmospheric uncertainties. The lack of a good estimate for these statistics can corrupt the trajectory reconstruction and lead to filter divergence. Herein lies the motivation for adaptive filtering, since one could gain information about the measurement and process noise parameters that could be helpful in updating the states and improve uncertainty quantification.

C. Adaptive filtering - covariance matching

As mentioned earlier, adaptive filtering is used when one does not have *a priori* accurate knowledge of the measurement and process noise. Unlike linear, discrete, stochastic problems where the best linear, minimum variance, unbiased estimate of the state is given by the Kalman filter, no optimal estimator is known for a case when the process noise and measurement noise parameters are unknown.[37] The approach used in this paper is the covariance matching or noise-adaptive technique and is summarized in Eqs. 3.[37,47]

$$w_j = \hat{x}_j - \bar{x}_j \quad j = 1, \ldots, N \tag{3a}$$

$$\hat{w} = \frac{1}{N} \sum_{j=1}^{N} w_j \tag{3b}$$

$$\hat{Q} = \frac{1}{N-1} \sum_{j=1}^{N} B \left[(w_j - \hat{w}) (w_j - \hat{w})^T - \left(\frac{N-1}{N} \right) \left(\bar{P}_j^* - \hat{P}_j \right) \right] B^T \tag{3c}$$

$$\bar{P}_j^* = \int_{t_{j-1}}^{t_j} \left(AP + PA^T \right) dt \tag{3d}$$

$$v_i = y_i - h(\bar{x}_i) \quad i = 1, \ldots, L \tag{3e}$$

$$\hat{v} = \frac{1}{L} \sum_{i=1}^{L} v_i \tag{3f}$$

$$\hat{R} = \frac{1}{L-1} \sum_{i=1}^{L} \left((v_i - \hat{v}) (v_i - \hat{v})^T - \left(\frac{L-1}{L} \right) H_i \bar{P}_i H_i^T \right) \tag{3g}$$

Since the exact process and measurement noise are unknown (together with the true states), empirically derived quantities serve as surrogates to estimate the process and measurement noise. The empirically derived quantities w and v are approximations of the actual state noise and measurement noise vectors. Using these quantities, one can estimate Q and R as shown in Eqs. 3. Information from the last N state estimates are used to calculate w, while information from the last L measurement points are used to calculate v.

The values for the various state and covariance updates are found from the EKF. The state noise vector's batch size N does not need to be the same as the measurement noise vector's batch size L. Also, it should be noted that for at least the first N and L state and measurement updates one has to use the *a priori* estimate of Q and R in the EKF. Thus, the batch sizes are tuning terms that need to be determined empirically: small batch sizes would mean that the filter can begin adapting quickly in the reconstruction process, but a small sample size also means that the estimated statistics, Q and R, are not representative according to the central limit theorem.

For the specific case of Mars EDL trajectory reconstruction, Q can give information about the aerodynamic coefficient uncertainties or the atmospheric property uncertainties on the day-of-the-flight. The measurement noise uncertainties, R, can give valuable information about the sensor calibration hitherto assumed to be known in reconstruction studies.

V. Results

A. Simulated Mars EDL trajectory

The Program to Optimize Simulated Trajectories II[48] is used to generate a Mars EDL trajectory for a 2.65 m diameter, 70 deg. sphere-cone that is shown in Figure 3. The vehicle characteristics are similar to that of the MER vehicles. This trajectory represents the truth data and the reconstructed values are compared with them.

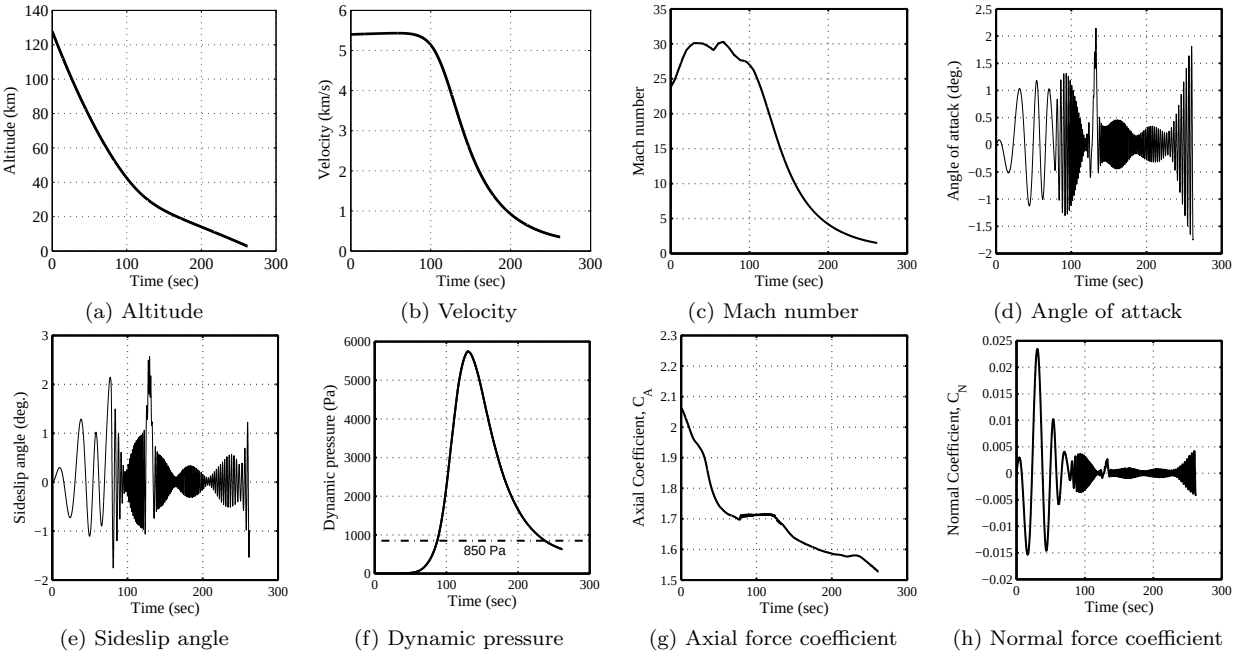

(a) Altitude (b) Velocity (c) Mach number (d) Angle of attack

(e) Sideslip angle (f) Dynamic pressure (g) Axial force coefficient (h) Normal force coefficient

Figure 3: Nominal reference trajectory used in the simulation.

Accelerometer, gyroscope, pressure transducer, and altimeter measurements are created using the simulated trajectory. Random noise is added to the simulated measurement and the sensors were effectively sampled at various frequencies to simulate the rate of data collected by a typical Mars EDL vehicle. The information is summarized in Table 3.

Table 3: Measurement noise uncertainties for the simulated dataset.

Measurement	3σ uncertainty (normal)	Sample rate (Hz.)	Availability
Three-axis sensed acceleration	100 μg-RMS[a]	100	Entire trajectory
Three-axis angular rate	0.03 deg/hour-RMS[b]	100	Entire trajectory
Radar altimeter altitude	0.3 m[a]	1	For alt. $\leq$ 10 km
Pressure transducers	1% reading/transducer[c]	8	Between 89-237 sec[d]

Notes: [a]Ref. 49 [b]Ref. 19 [c]Ref. 11 [d] When dynamic pressure is above a threshold (850 Pa)

The random noise statistic is also used for the measurement noise covariance in this case. Although the adaptive filtering method described in the earlier section can calculate the measurement noise covariance from the residual of the outputs, this study is focused on estimating the process noise covariance more accurately to improve the uncertainty quantification of the states. In previous studies,[10,31] it has been seen that model errors, especially of the atmospheric and aerodynamic parameters, can drive the overall uncertainty of the states, and thus they are the main objectives of this study. In a real Mars flight case, measurement uncertainty can also degrade due to the sensor's exposure to extreme space conditions, but for this study that uncertainty has been assumed to be known. Future work could include estimation with unknown measurement noise. Statistical filtering also requires the knowledge of the initial state covariance. This information for the current example is summarized in Table 4, which is based on initial state covariances

of recent planetary entry missions.

Table 4: Initial state uncertainties used for the reconstruction process.

State	3σ uncertainty (normal)
Radius (planet-centric)[49]	5100 m
Latitude (planet-centric)[49]	0.12 deg.
Longitude[49]	0.03 deg.
Velocity (relative)[19]	2.9 m/s
Flight path angle (relative)[49]	0.06 deg.
Heading angle (relative)[49]	0.06 deg.
Euler angles (related to the quaternion)	0.03 deg./angle
Freestream pressure	$10P_{\infty,0}$
Freestream density	$10\rho_{\infty,0}$

B. Reconstruction Results

Figure 4 compares the reconstructed trajectory using the adaptive filtering technique to the actual data. One can see that there is a close agreement between the estimated and actual quantities. The maximum error in altitude is only around 150 m and the maximum velocity error is about 0.5 m/s throughout an EDL sequence that lasts around 275 seconds. Interestingly, the effect of the relatively low uncertainty radar altimeter data is clearly visible in the altitude plots when the residual of the error reduces significantly around 220 seconds when that data are introduced. This is very similar to actual Mars EDL cases when radar altimeter data available during terminal landing greatly reduces the error ellipse of the landing site derived from accelerometer only data.[28,31]

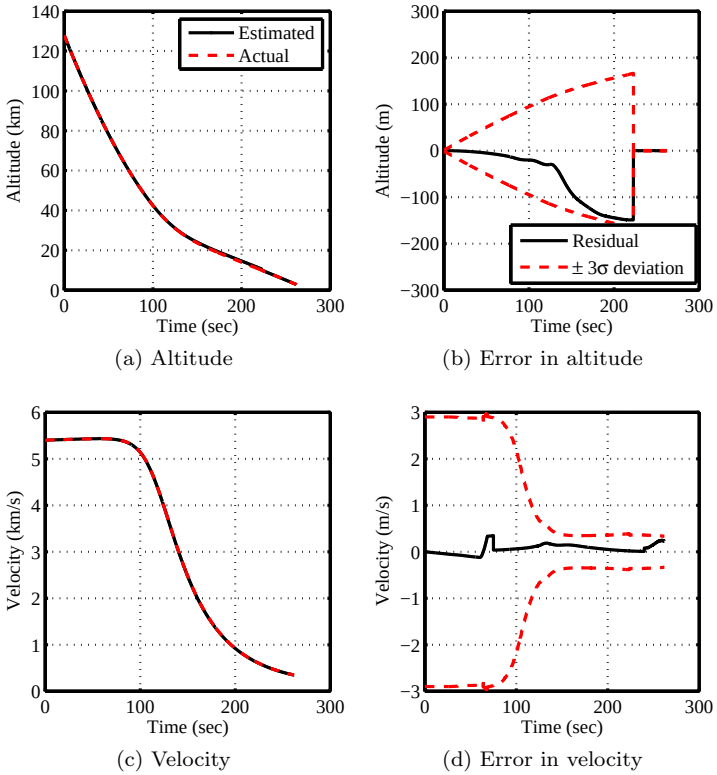

(a) Altitude (b) Error in altitude

(c) Velocity (d) Error in velocity

Figure 4: Estimated position and velocity using adaptive filter (N = 10).

Some derived states, such as angle of attack, sideslip angle, and dynamic pressure, are also important

in EDL performance evaluation and can be calculated using a combination of the estimated state vector. These reconstructed states are shown in Figure 5.

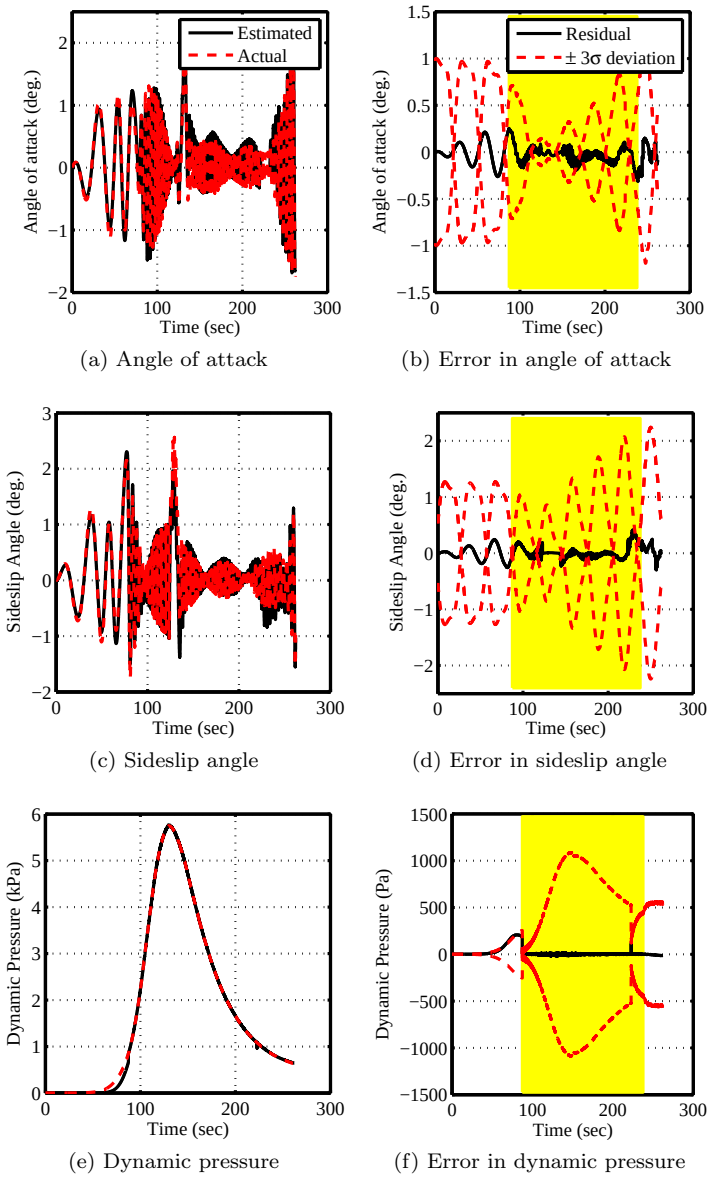

(a) Angle of attack (b) Error in angle of attack

(c) Sideslip angle (d) Error in sideslip angle

(e) Dynamic pressure (f) Error in dynamic pressure

Figure 5: Derived trajectory and atmospheric parameters using adaptive filter (N = 10) estimation results.

In Fig. 5, the yellow band shows the region when pressure transducer measurements were available. It has been noted before that typical Mars EDL dataset often leave many parameters of interest directly unobservable. However, FADS sensors measure the pressure distribution on the aeroshell during entry, which in turn can be used to estimate freestream density and pressure without relying solely on accelerometer data. This additional source of information also has the effect of improving the estimation of quantities like angle of attack and dynamic pressure, which can be observed in a slight improvement in the residual after the introduction of this data. The adaptive filter further improves the uncertainty estimation of these parameters, which is signified by the tight confidence bounds of the estimated states when compared to uncertainty quantification results obtained using other statistical filters. The performance of non-adaptive statistical filters for the same simulated data can be found in Ref. 10, and the comparison of some of the state and uncertainty estimation performance is summarized in Table 5 and Fig. 8 later in this paper.

Finally, adaptive filters provide another benefit by quantifying uncertainties of underlying process model parameters, such as aerodynamic coefficients. Figure 6 shows the reconstructed axial force coefficient compared to the actual aerodynamic coefficient value. One can see that the introduction of the pressure data

immediately improves the reconstruction accuracy. More importantly, the estimated axial force coefficient's uncertainties are tightly bound in this region, at least when compared to the results of other statistical filters.[10] The tighter confidence bounds raises hope that reconstruction of actual flight data using adaptive filters will give realistic confidence bounds for estimated force coefficient and possibly allow for the maturation of current aerodynamic error models (such as those shown in Table 1).

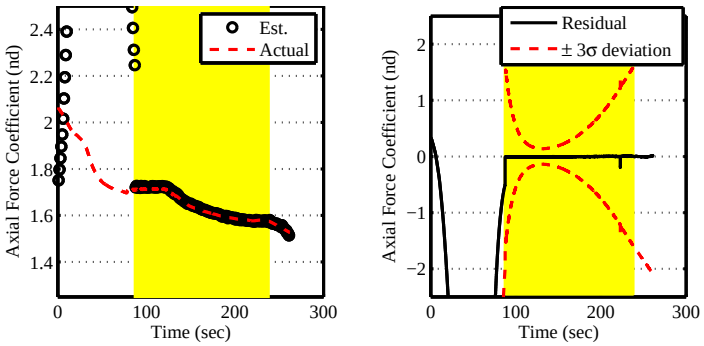

(a) Axial force coefficient (b) Axial force coefficient error

Figure 6: Derived aerodynamic parameter using adaptive filter (N = 10) estimation results.

C. Tuning of the Adaptive Filter

Most statistical filters have tuning parameters that have to be determined by the analyst to ensure that the filter maintains consistency and does not diverge. For Extended Kalman Filters, the tuning parameters are usually process noise, which the analyst determines experimentally or by using an optimization procedure.[50] An Adaptive filter with the covariance matching technique takes this subjectivity out of the equation by using the state and measurement residual statistics to calculate process and measurement noise and thus ensure consistency. However, since sample statistics are substituted for true (but unknown) statistics of the problem, there is still some subjectivity left in the choice of the sample size. Too large of a sample size will ignore sudden changes in the process dynamics, while too small of a sample size will not be consistent with the central limit theorem and produce oscillatory results. One can compare this situation to using a moving average filter with a variable sample window.

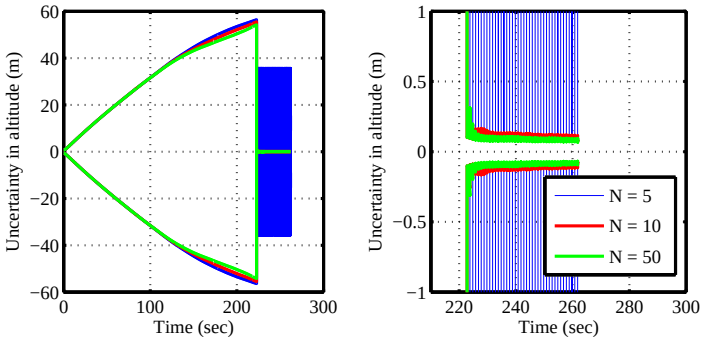

(a) Effect of N (b) Zoomed-in look

Figure 7: Effect of the adaptive filter batch size on uncertainty calculation.

Myers[37] recommends using a fading memory weighting factor to emphasize recent samples in the statistical calculation. However, this introduces another subjective tuning parameter for the analyst to choose. Additionally, experimentally this filter has been found to be useful for situations when there is a sudden shift in dynamics, such as a vehicle maneuver. For the simulated EDL dataset used for this study, there are no such sudden maneuvers; thus, the fading memory filter was not utilized. It may be useful, however, for the reconstruction of other types of EDL datasets, such as MSL, which has several bank angle reversals.

Thus, the only tuning parameter was the batch sample size, N, which was found experimentally as shown in Fig. 7. The filter was run for several N-values, and it was found that N = 10 provides uncertainty values

consistent with filters with much larger N-values. Note that for a small sample size of N = 5, the uncertainty values are very oscillatory, especially during the terminal descent region where a highly certain altimeter data and a relatively less certain accelerometer data are available. With a small sample size, the uncertainty oscillates between the altitude estimate from these two data sources.

D. Comparison of Estimation Performance

The benefit of using adaptive filtering is more apparent when compared with results from other statistical filters with subjectively-derived process noise. Table 5 shows a comparison of the state estimation results from the Adaptive Filter abnd results from the EKF and Unscented Kalman Filter (UKF) found in a previous study using the same simulated dataset.[10] Figure 8 shows a similar comparison for the uncertainty estimation.

Table 5: Comparison of state estimation performance between EKF, UKF, and Adaptive Filter.[a]

State	EKF	UKF	Adaptive
Angle of attack (deg.)	0.192	0.145	0.082
Sideslip angle (deg.)	0.211	0.140	0.112
Dyn. pressure (% max pressure)[b]	0.670	0.283	0.081
Axial force coefficient	0.017	0.006	0.005

[a]RMS of the residual when FADS is available.

[b]RMS residual normalized by max. pressure and turned to a percentage.

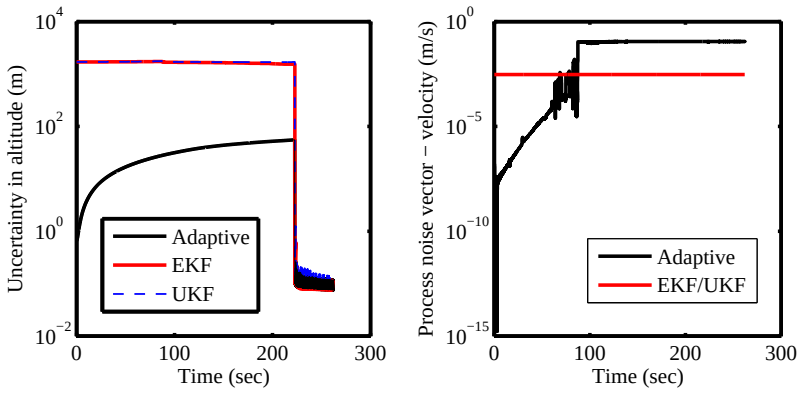

(a) Altitude uncertainty (b) Process noise for velocity

Figure 8: State uncertainty quantification comparison between EKF, UKF, and Adaptive filter.

Adaptive filtering provides marked improvement in state estimation, as demonstrated by the low root mean square (RMS) of the residuals. However, the biggest benefit is in the tighter confidence bounds as seen in Fig. 8a. The process noise used for the EKF and UKF to have non-divergent solutions was chosen to be an uniform value using auto-tuning techniques found in Ref. 50. However, the adaptively calculated process noise varied over time (as seen in Fig. 8b) and was sometimes greater than and less than the process noise used for the EKF and UKF. This adaptive noise allowed the filter to have the appropriate level of noise necessary to maintain consistency and accuracy in the state estimation without increasing the state uncertainty too much. The result was a more accurate state estimation with tighter confidence bounds.

VI. Conclusions

Mars entry, descent, and landing vehicle trajectories are highly dependent on the vehicle aerodynamic coefficients and the atmospheric properties on the day-of-flight. These parameters are hard to simulate and test on Earth, and despite seven successful entry, descent, and landing missions, there remains high uncertainty in the knowledge of these parameters. Traditional entry, descent, and landing reconstructions have either deterministically estimated the vehicle's trajectory, thus ignoring measurement and model uncertainties, or

have assumed *a priori* knowledge of the process and measurement noise vectors in the statistical filter. Adaptive filtering techniques discussed in this paper can estimate these unknown parameters together with the state vector of the statistical filter. This methodology is tested here with simulated Mars entry trajectories (where truth data are known) to improve the estimation of the vehicle's trajectory, atmosphere, and aerodynamic coefficients as well as the uncertainties associated with these parameters. The results show a marked improvement in state estimation using covariance matching adaptive filter techniques when compared with other statistical filters, such as the Extended Kalman Filter and the Unscented Kalman Filter. However, the best improvement is in the significantly tighter confidence bounds calculated during the uncertainty quantification process. This leads one to believe that adaptive filters can give realistic uncertainty values when actual flight data are reconstructed. These estimated states and uncertainties can further improve the current engineering models of vehicle aerodynamics and Martian atmosphere.

Acknowledgments

The Space Systems Design Laboratory at the Georgia Institute of Technology developed the tools used in this paper. NASA Research Announcement (NRA) award No. NNX12AF94A has supported this research. The authors want to thank Bernie Laub of NASA Ames Research Center and Mark Schoenenberger and Scott Striepe of NASA Langley Research Center for their advice and help.

References

[1]Striepe, S., Way, D., Dwyer, a. M., and Balaram, J., "Mars Science Laboratory Simulations for Entry, Descent, and Landing," *Journal of Spacecraft and Rockets*, Vol. 43, No. 2, March 2006, pp. 311–323.

[2]Schoenenberger, M., Dyakonov, A. A., Buning, P., Scallion, W., and Van Norman, J., "Aerodynamic Challenges for the Mars Science Laboratory Entry, Descent and Landing," AIAA 2009-3914, *AIAA Thermophysics Conference,* San Antonio, TX, 2009.

[3]Edquist, K. T., Desai, P. N., and Schoenenberger, M., "Aerodynamics for the Mars Phoenix Entry Capsule," *Journal of Spacecraft and Rockets*, Vol. 48, No. 3, 2011, pp. 713–726.

[4]Edquist, K., "Computations of Viking Lander Capsule Hypersonic Aerodynamics with Comparisons to Ground and Flight data," AIAA-2006-6137, *AIAA Atmospheric Flight Mechanics Conference and Exhibit,* Keystone, CO, No. August, 2006.

[5]Desai, P. N., Blanchard, R. C., and Powell, R. W., "Entry trajectory and atmosphere reconstruction methodologies for the Mars Exploration Rover mission," *International Planetary Probe Workshop*, 2004.

[6]Justus, C. and Johnson, D., "Mars Global Reference Atmosphere Model, 2001 Version (Mars-GRAM 2001): Users Guide," Tech. rep., NASA TM-210961, 2001.

[7]Tyler, D., Barnes, J., and Haberle, R., "Simulation of surface meteorology at the Pathfinder and VL1 sites using a Mars mesoscale model," *Journal of Geophysical Research*, Vol. 107, No. E4, 2002.

[8]Vasavada, A., Chen, A., Barnes, J., Burkhard, P., Canton, B., Dwyer-Cianciolo, A., Fergason, R., Hinson, D., Justh, H., Kass, D., Lewis, S., Mischna, M., Murphy, J., Rakfin, S., Tyler, D., and Withers, P., "Assessment of Environments for Mars Science Laboratory Entry, Descent, and Surface Operations," *Space Science Review*, 2012.

[9]Chen, A., Vasavada, A., Cianciolo, A., Barnes, J., Tyler, D., Rafkin, S., Hinson, D., and Lewis, S., "Atmospheric Risk Assessment for the Mars Science Laboratory Entry, Descent, and Landing System," IEEEAC 1153, *IEEE Aerospace Conference,* Big Sky, MT, 2010.

[10]Dutta, S., Braun, R. D., Russell, R. P., Clark, I. G., and Striepe, S. A., "Comparison of Statistical Estimation Techniques for Mars Entry, Descent, and Landing Reconstruction from MEDLI- like Data Sources," AIAA 2012-0400, *AIAA Aerospace Sciences Meeting,* Nashville, TN, 2012.

[11]Gazarik, M. J., Wright, M. J., Little, A., Cheatwood, F. M., Herath, J. A., Munk, M. M., Novak, F. J., and Martinez, E. R., "Overview of the MEDLI Project," IEEEAC 1510, *IEEE Aerospace Conference,* Big Sky, MT, 2008.

[12]Ingoldby, R., Michel, F., Flaherty, T., Doty, M., Preston, B., Villyard, K., and Steele, R., "Entry Data Analysis for Viking Landes 1 and 2," Tech. rep., NASA CR 159388, 1976.

[13]Euler, E., Adams, G., and Hopper, F., "Design and Reconstruction of the Viking Lander Descent Trajectories," *Journal of Guidance, Control, and Dynamics*, Vol. 1, No. 5, 1978, pp. 372–378.

[14]Spencer, D., Blanchard, R., Braun, R., Kallemeyn, P., and Thurman, S., "Mars Pathfinder Entry, Descent, and Landing Reconstruction," *Journal of Spacecraft and Rockets*, Vol. 36, No. 3, 1999, pp. 348–356.

[15]Schofield, J. T., Barnes, J., Crisp, D., Haberle, R., Larsen, S., Magalhaes, J., Murphy, J., Seiff, A., and Wilson, G., "The Mars Pathfinder Atmospheric Structure Investigation/Meteorology (ASI/MET) Experiment," *Science*, Vol. 278, No. 5344, Dec. 1997, pp. 1752–1758.

[16]Blanchard, R. C., "Entry, Descent, and Landing Trajectory and Atmosphere Reconstruction for the Mars Exploration Rovers Missions A and B," Tech. rep., NASA-JPL Subcontract CCNS20568F, 2008.

[17]Withers, P. and Smith, M., "Atmospheric entry profiles from the Mars Exploration Rovers Spirit and Opportunity," *Icarus*, Vol. 185, No. 1, Nov. 2006, pp. 133–142.

[18]Desai, P. N., Prince, J. L., Queen, E. M., Schoenenberger, M., Cruz, J. R., and Grover, M. R., "Entry, Descent, and Landing Performance of the Mars Phoenix Lander," *Journal of Spacecraft and Rockets*, Vol. 48, No. 5, 2012, pp. 798–808.

[19]Blanchard, R. C. and Desai, P. N., "Mars Phoenix Entry , Descent , and Landing Trajectory and Atmosphere Reconstruction," *Journal of Spacecraft and Rockets*, Vol. 48, No. 5, 2012, pp. 809–821.

[20]Steltzner, A., Kipp, D., Chen, A., Burkhart, D., Guernsey, C., Mendeck, G., Mitcheltree, R., Powell, R., Rivellini, T., Martin, M. S., and Way, D., "Mars Science Laboratory Entry, Descent, and Landing System," IEEEAC 1497, *IEEE Aerospace Conference,* Big Sky, MT, 2006.

[21]Jones, J., "Development and Performance Analysis of a Trajectory Estimator for an Entry Through the Martian Atmosphere," AIAA 1972-953, 1972.

[22]Sabin, M. L., "Linear Filtering of Ballistic-Entry Probe Data For Atmospheric Reconstruction," *Journal of Spacecraft and Rockets*, Vol. 12, No. 2, Feb. 1975, pp. 66–73.

[23]Hopper, F., "Trajectory, Atmosphere, and Wind Reconstruction from Viking Measurement," AAS 75-068, *AIAA/AAS Astrodynamics Conference,* Nassau, Bahama, 1975.

[24]Compton, H., Findlay, J., Kelly, G., and Heck, M., "Shuttle (STS-1) Entry Trajectory Reconstruction," AIAA 1981-2459, *AIAA/SETP/SFTE/SAE/ITEA/IEEE Flight Testing Conference,* Las Vegas, NV, 1981.

[25]Karlgaard, C., Blanchard, R., Kirsch, M., Tartabini, P., and Toniolo, M., "Hyper-X Post-Flight Trajectory Reconstruction," *Journal of Spacecraft and Rockets*, Vol. 43, No. 1, Jan. 2006, pp. 105–115.

[26]Karlgaard, C. D., Beck, R. E., Keefe, S. A., Siemers, P. M., White, B. A., Engelund, W. C., and Munk, M. M., "Mars Entry Atmospheric Data System Modeling and Algorithm Development," AIAA 2009-3916, *AIAA Thermophysics Conference,* San Antonio, TX, 2009.

[27]Karlgaard, C., Beck, R., Derry, S., Brandon, J., Starr, B., Tartabini, P., and Olds, A., "Ares I-X Best Estimated Trajectory and Comparison with Preflight Predictions," AIAA 2011-6466, *AIAA Atmospheric Flight Mechanics Conference,* Portland, OR, 2011.

[28]Christian, J. A., *Statistical Reconstruction of Mars Entry, Descent, and Landing Trajectories and Atmospheric Profiles*, Master's thesis, Georgia Institute of Technology, 2007.

[29]Wells, G. and Braun, R. D., "Reconstruction of the Spirit Mars Exploration Rover Entry, Descent and Landing Performance," AA 3-2008-16, *International ARA Days Conference,* Arachon, France, 2008.

[30]Wells, G., *A Comparison of Multiple Techniques for the Reconstruction of Entry, Descent, and Landing Trajectories and Atmospheres*, Ph.D. thesis, Georgia Institute of Technology, 2011.

[31]Dutta, S. and Braun, R., "Mars Entry, Descent, and Landing Trajectory and Atmosphere Reconstruction," AIAA 2010-1210, *AIAA Aerospace Sciences Meeting,* Orlando, FL, 2010.

[32]Dutta, S., Clark, I., Russell, R., and Braun, R., "Statistical Entry, Descent, and Landing Performance Reconstruction of the Mars Phoenix Lander," *International Planetary Probe Workshop, Portsmouth, VA*, 2011.

[33]Fitzgerald, R., "Divergence of the Kalman Filter," *IEEE Transactions on Automatic Contro*, Vol. 16, No. 6, 1971, pp. 736–747.

[34]Mehra, R., "Approaches to adaptive filtering," *IEEE Transactions on Automatic Control*, Vol. 17, No. 5, Oct. 1972, pp. 693–698.

[35]Magill, D., "Optimal Adaptive Estimation of Sampled Stochastic Processes," *IEEE Transactions on Automatic Control*, Vol. 10, No. 4, 1965, pp. 434–439.

[36]Tapley, B. D. and Born, G. H., "Sequential Estimation of the State and the Observation-Error Covariance Matrix," *AIAA Journal*, Vol. 9, No. 2, 1971, pp. 212–217.

[37]Myers, K. and Tapley, B. D., "Adaptive sequential estimation with unknown noise statistics," *IEEE Transactions on Automatic Contro*, Vol. 21, No. 4, 1976, pp. 520–523.

[38]Maybeck, P., Jensen, R., and Harnly, D., "An Adaptive Extended Kalman Filter for Target Image Tracking," *IEEE Transactions on Aerospace and Electronic Systems*, Vol. AES-17, No. 2, March 1981, pp. 173–180.

[39]Whitmore, S. and Leondes, C., "Formulation and Implementation of a Practical Algoritm for Non-Stationary Adaptive State Estimation," *International Journal of Control*, Vol. 44, No. 3, 1986, pp. 767–775.

[40]Hull, D. G., Speyer, J. L., and Greenwell, W. M., "Adaptive Noise Estimation for Homing Missiles," *Journal of Guidance*, Vol. 7, No. 3, 1983, pp. 322–328.

[41]Chu, Q., Mulder, J., and van Woerkom, P., "Modified Recursive Maximum Likelihood Adaptive Filter for Nonlinear Aircraft Flight-Path Reconstruction," *Journal of Guidance, Control, and Dynamics*, Vol. 19, No. 6, 1996, pp. 1285–1295.

[42]Mendonca, C. B. D., Hemerly, E. M., and Goes, L. C. S., "Adaptive Stochastic Filtering for Online Aircraft Flight Path Reconstruction," *Journal of Aircraft*, Vol. 44, No. 5, Sept. 2007, pp. 1546–1558.

[43]Marschke, J. M., Crassidis, J. L., and Lam, Q. M., "Multiple Model Adaptive Estimation for Inertial Navigation During Mars Entry," AIAA 2008-7352, *AIAA/AAS Astrodynamics Specialist Conference and Exhibit,* Honolulu, HI, 2008.

[44]Vinh, N., Busemann, A., and Culp, R., *Hypersonic and Planetary Entry Flight Mechanics*, The University of Michigan Press, Ann Arbor, MI, 1980.

[45]Kuipers, J., *Quaternions and Rotation Sequences*, Princeton University Press, Princeton, NJ, 1999.

[46]Zarchan, P. and Musoff, H., *Fundamentals of Kalman Filtering, A Practical Approach*, American Institute of Aeronautics and Astronautics, Reston, VA, 2000.

[47]Stengel, R., *Optimal Control and Estimation*, Dover Publications, New York, NY, 1994.

[48]Striepe, S., Powell, R., Desai, P., Queen, E.M., B. G., Cornick, D., Olson, D., and Peterson, F., *Program To Optimize Simulated Trajectories (POST II), Vol. II: Utilization Manual,* Version 1.1.6.G, 2004.

[49]Christian, J., Verges, A., and Braun, R., "Statistical Reconstruction of Mars Entry, Descent, and Landing Trajectories and Atmospheric Profiles," AIAA 2007-6192, *AIAA SPACE Conference and Exposition,* Long Beach, CA, 2007.

[50]Powell, T., "Automated Tuning of an Extended Kalman Filter Using the Downhill Simplex Algorithm," *Journal of Guidance, Control, and Dynamics*, Vol. 25, No. 5, 2002, pp. 901–908.